Angewandte
International Edition Chemie

DOI: 10.1002/anie.201209911

Sustainable Catalysis

The Electronic States of Rhenium Bipyridyl Electrocatalysts for CO_2 Reduction as Revealed by X-ray Absorption Spectroscopy and Computational Quantum Chemistry**

*Eric E. Benson, Matthew D. Sampson, Kyle A. Grice, Jonathan M. Smieja, Jesse D. Froehlich, Daniel Friebel, John A. Keith, Emily A. Carter, Anders Nilsson, and Clifford P. Kubiak**

Industrial processes and fossil fuel combustion produce carbon dioxide (CO_2) unsustainably on the gigaton scale. Addressing this pressing issue has led to rapidly growing efforts to catalytically reduce CO_2 to liquid fuels.[1] Recycling CO_2 is a profoundly challenging problem that requires fundamental insights to guide advancements. Information regarding CO_2 transformations abound,[1,2] but no industrial-scale process has capably reduced CO_2 to liquid fuels. Of the systems that electrocatalytically reduce CO_2, the [Re(bpy)$(CO)_3$Cl] family of compounds (bpy = 2,2′-bipyridine) is one of the most robust and well-characterized systems known to date.[2a,3] This system converts CO_2 into carbon monoxide (CO) with high rates and efficiencies; it suffers, however, from large overpotentials that are believed to arise from accessing the highly reduced, formally Re^{-I} state in $[Re(bpy)(CO)_3]^-$. This state has long been proposed as the active state of the electrocatalyst.[3a,b,d] Apart from this assumption, there is little known about the electronic structure of the catalyst in its reduced (active) state and its subsequent interaction with CO_2.

We recently reported stopped-flow kinetics studies showing the relative selectivities of the $[Re(bpy\text{-}t\mathrm{Bu})(CO)_3]^-$ anion reacting with with CO_2 and proton sources. These studies revealed that reaction rates of the anion were about 35 times faster with CO_2 than with weak acid.[3b] The bpy ligand was proposed to play a non-innocent role by storing charge and preventing a doubly occupied d_{z^2} orbital at the Re center, which would be needed to form a metal hydride. Indeed, X-ray diffraction (XRD) studies of both $[Re(bpy)(CO)_3]^-$ and $[Re(bpy\text{-}t\mathrm{Bu})(CO)_3]^-$ show the bpy ligands exhibit bond length alternation and short C_{py}–C_{py} bonds (1.370(15) Å, for bpy-*t*Bu), indicating significant electron density on these ligands. The short inter-ring bonds suggest a doubly reduced bpy ligand,[4] more representative of a $Re^{+I}(bpy^{2-})$ state rather than a $Re^{0}(bpy^{-})$ or $Re^{-I}(bpy^{0})$ state. The redox activities of bpy ligands[4,5] as well as other non-innocent ligands have been extensively studied.[6]

To fully confirm that the non-innocence of bpy contributes to this unique catalysis, we employed experimental spectroscopy and theoretical quantum chemistry to characterize this catalyst family. We compared the halide starting materials, [Re(bpy)$(CO)_3$Cl] (**1**) and [Re(bpy-*t*Bu)$(CO)_3$Cl] (**2**), the one-electron reduced dimer $[\{Re(bpy)(CO)_3\}_2]$ (**3**), the two-electron reduced anions [K([18]crown-6)][Re(bpy)$(CO)_3$] (**4**) and [K([18]crown-6)][Re(bpy-*t*Bu)$(CO)_3$] (**5**), the commercially available standards, [Re$(CO)_5$Cl] (**6**) and $[Re_2(CO)_{10}]$ (**7**), and a synthesized Re^{-I} standard, [K([18]crown-6)][Re$(CO)_5$] (**8**). IR spectroscopy of the stretching frequencies of the carbonyl ligands characterizes the electronic states of these complexes. X-ray absorption spectroscopy (XAS) at the Re L_3 absorption edge using the strong "white-line" resonance arising from 2p→5d transitions probes the Re 5d unoccupied states. Kohn–Sham density functional theory (KS-DFT) calculations provide a first-principles description of electronic structures. Lastly, extended X-ray absorption fine structure (EXAFS) studies of frozen THF solutions of **1**, **2**, **4**, and **5** confirm the monomeric nature of the catalysts and rule out solvent coordination to the Re centers in solution.

Compounds **1**–**5** were prepared according to literature procedures.[3a,b,d] [K([18]crown-6)][Re$(CO)_5$] (**8**) was prepared by the reduction of $[Re_2(CO)_{10}]$ (**7**) in tetrahydrofuran (THF) by excess KC_8 (potassium intercalated graphite) in the presence of [18]crown-6 (see the Supporting Information).

The IR stretching frequencies of complexes **1**–**7** have been reported previously;[3a,b,d,7] however, we obtained frequencies for complexes **1**–**7** and the newly synthesized complex **8** under the same conditions for fair comparison (Table 1). The one-electron reduction of the formally Re^{+I} chloride species **2** results in formation of the one-electron reduced monomer,

---

[*] Dr. E. E. Benson,[+] M. D. Sampson,[+] Dr. K. A. Grice,
Dr. J. M. Smieja, J. D. Froehlich, Prof. Dr. C. P. Kubiak
Department of Chemistry and Biochemistry, University of California, San Diego
9500 Gilman Drive,Code 0358, La Jolla, CA 92093-0358 (USA)
E-mail: ckubiak@ucsd.edu

Dr. D. Friebel, Prof. Dr. A. Nilsson
SLAC National Accelerator Laboratory
2575 Sand Hill Road, Menlo Park, CA 94025 (USA)

Dr. J. A. Keith, Prof. Dr. E. A. Carter
Department of Mechanical and Aerospace Engineering, Princeton University
D404A Engineering Quadrangle, Princeton, NJ 08544 (USA)

[+] These authors contributed equally to this work.

[**] This material is based upon work supported by the Air Force Office of Scientific Research through the MURI program under AFOSR Award No. FA9550-10-1-0572. This research was partly carried out at the Stanford Synchrotron Radiation Lightsource, a National User Facility operated by Stanford University on behalf of the U.S. Department of Energy, Office of Basic Energy Sciences. We thank John Bargar, Matthew Latimer, Erik Nelson, and Juan Lezama Pacheco for their support of the X-ray Absorption Spectroscopy experiments. We also thank Dr. Arnold Rheingold and Dr. Curtis Moore for their assistance with the single crystal XRD experiments.

Supporting information for this article is available on the WWW under http://dx.doi.org/10.1002/anie.201209911.

© 2013 Wiley-VCH Verlag GmbH & Co. KGaA, Weinheim

Table 1: IR stretching frequencies for selected compounds.

Compound	ν(CO) [cm^{-1}]
[Re(bpy)(CO)$_3$Cl] (**1**)[a]	2019, 1918, 1894
[Re(bpy-*t*Bu)(CO)$_3$Cl] (**2**)[a]	2018, 1915, 1890
[Re(bpy)(CO)$_3$Cl]$^-$[b]	1998, 1880, 1866
[{Re(bpy)(CO)$_3$}$_2$] (**3**)[a]	1991, 1951, 1885, 1862
[Re(bpy)(CO)$_3$]$^-$ (**4**)[a]	1945, 1839 (br)
[Re(bpy-*t*Bu)(CO)$_3$]$^-$ (**5**)[a]	1940, 1835 (br)
[Re(CO)$_5$Cl] (**6**)[a]	2041, 1980 (br)
[Re$_2$(CO)$_{10}$] (**7**)[a]	2070, 2010, 1966
[Re(CO)$_5$]$^-$ (**8**)[a]	1907, 1861 (br)

[a] IR stretching frequencies for these compounds were obtained for this study (THF). [b] IR stretching frequencies were taken from Ref. [8] (CH$_3$CN).

[Re(bpy)(CO)$_3$Cl]$^-$, which has been previously characterized spectroscopically (Table 1).[3d,8] This reduction results in a shift of about 21 cm^{-1} in the high-energy band and has been previously attributed to formation of a bpy radical.[3d,8] This species has not been isolated and quickly converts into the [{Re(bpy)(CO)$_3$}$_2$] dimer (**3**). The two-electron reduction of the formally Re^{+I} chloride species (**1** and **2**) to the anionic species (**4** and **5**) results in a shift of about 75 cm^{-1} in the high-energy band. This has been previously attributed to the formation of a Re^0(bpy$^-$) state.[3b] In contrast, the two-electron reduction of standard **6** to its anionic state **8** results in a shift of 134 cm^{-1}. This larger shift in the carbonyl stretching frequencies can be attributed to the formation of a Re^{-I} formal oxidation state, as the [Re(CO)$_5$]$^-$ anion lacks a redox-active ligand to store additional charge.

Compounds **1**–**5** have been crystallized previously.[3a,b,9] Table 2 lists relevant bond lengths for compounds **1**, **2**, **4**, and **5** (see below). Reduction of the dimer **7** using KC$_8$ results in the formation of the five-coordinate rhenium anion [K([18]crown-6)][Re(CO)$_5$] (**8**). XRD quality crystals of complex **8** were grown from the vapor diffusion of *n*-hexane into a solution of the complex in THF (Supporting Information, Figure S1). Crystal data and structure refinement information for complex **8** are listed in the Supporting Information, Table S1.

Table 2: Coordination numbers (C.N.) and bond distances [Å] for compounds **1**, **2**, **4**, and **5**.

Compound		EXAFS	XRD[a]	Ref.
[Re(bpy)(CO)$_3$Cl] (**1**)	C.N.	6.1(2)	6	[9a]
	Re–C	1.93(2)	1.930(8)	
	Re–N	2.18(5)	2.175(6)	
	Re–Cl	2.49(2)	2.460(2)	
[Re(bpy-*t*Bu)(CO)$_3$Cl] (**2**)	C.N.	6.2(2)	6	[9b]
	Re–C	1.92(1)	1.911(4)	
	Re–N	2.17(4)	2.176(3)	
	Re–Cl	2.49(2)	2.463(1)	
[Re(bpy)(CO)$_3$]$^-$ (**4**)	C.N.	4.9(2)	5	[3a]
	Re–C	1.91(2)	1.892(5)	
	Re–N	2.14(2)	2.082(4)	
[Re(bpy-*t*Bu)(CO)$_3$]$^-$ (**5**)	C.N.	5.1(2)	5	[3b]
	Re–C	1.91(2)	1.917(10)	
	Re–N	2.14 (2)	2.093(7)	

[a] Averages of values found in the unit cell.

XAS at the Re L_3 edge were collected at SSRL beam line 4–1 for compounds **1**–**8**. XAS of low-valence Re complexes containing carbonyl ligands exhibit extraordinarily strong white lines that resemble Re oxides much more than metallic Re^0.[10] This is attributed to metal d orbitals coupling to empty π* orbitals of the carbonyl ligands; this generates additional unoccupied states with partial Re 5d character that would not exist in purely σ-bonded compounds or in Re metal.

Figure 1 shows a comparison of the XAS white-line region for the standards **6**–**8**. The white-line intensity decreases as expected with decreasing formal oxidation state of the Re center. In contrast, when considering a series of Re bipyridyl complexes formally charged as Re^{+I}, Re^0, and Re^{-I}, we observe a marked decrease of the white-line intensity for the first reduction step from **1**→**3** (Figure 2a), but not for the second reduction step from **3**→**4** (Figure 2b). The two-electron reduction of the bpy-*t*Bu complex **2**→**5** also has a similar spectral change as that for **1**→**4** (Supporting Information, Figures S3 and S2, respectively). This indicates the metal center in the anionic rhenium complexes possess similar electronic states as the Re^0 dimer **3** (Figure 2b).

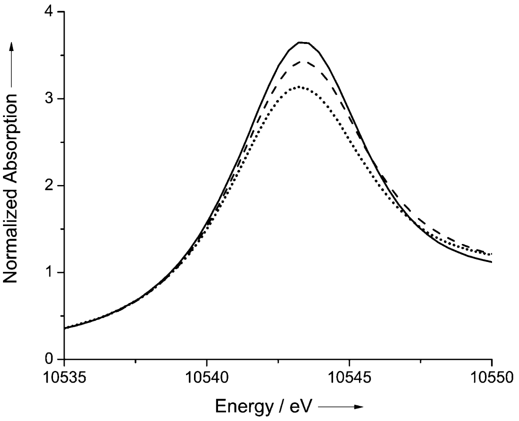

Figure 1. Comparison of the XAS white line regions for **6** (——), **7** (-----), and **8** (•••••).

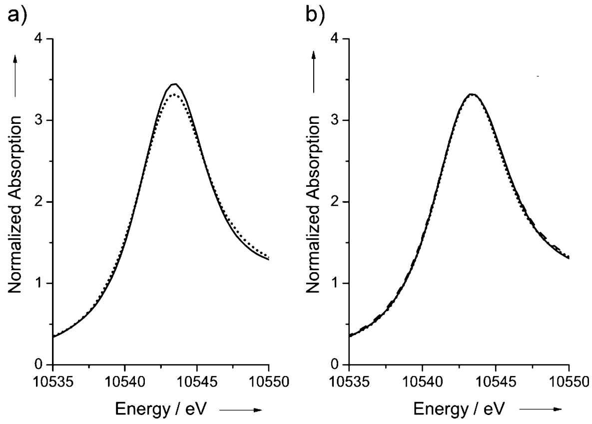

Figure 2. a) XAS white line regions for complexes **1** (——) and **3** (•••••). b) XAS white line regions for complexes **3** (——), **4** (-----), and **5** (•••••), showing no change in features.

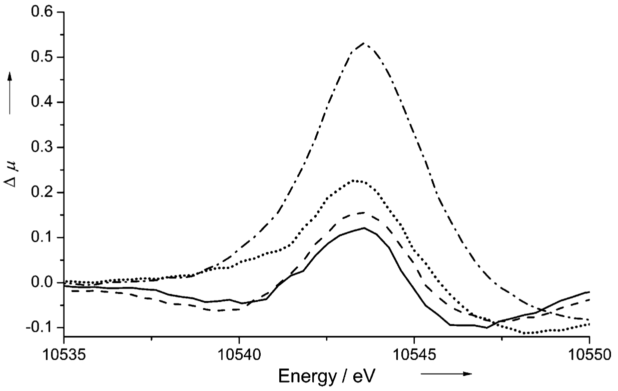

Figure 3. XANES difference spectra for the Re$^+$ complexes **1** and **2** and their corresponding anionic complexes **4** and **5** ($\Delta\mu$ is the change in normalized absorption). The [Re(bpy)(CO)$_3$] pair (**1**, **4**) is shown as (——), and the [Re(bpy-*t*Bu)(CO)$_3$] pair (**2**, **5**) is shown as (-----). For reference, the difference in XANES spectra for [Re(CO)$_5$Cl] (**6**) and [Re$_2$(CO)$_{10}$] (**7**) is shown as (•••••), and the difference spectra for [Re(CO)$_5$Cl] (**6**) and [Re(CO)$_5$]$^-$ (**8**) is shown as (–•–•).

Figure 3 shows reduction-induced white-line intensity changes in more detail. We compare the white line intensity decrease for reduction of standard **6**→**7**, and the two-electron reductions of the chloride compounds **1** and **2** to the anions **4** and **5**, respectively. The difference spectra $\mu(\mathbf{6})-\mu(\mathbf{7})$ and $\mu(\mathbf{6})-\mu(\mathbf{8})$ (where μ is a normalized absorption coefficient) represent the Re^{+I}→Re^0 and Re^{+I}→Re^{-I} reductions, respectively. Note, however, that changes in the Re 5d–CO π* coupling will inevitably accompany the oxidation state and symmetry changes and in turn will contribute additional small changes to the white-line and overlapping multiple-scattering resonances. The latter complication limits the accuracy of counting 5d vacancies by integrating $\Delta\mu$. However, the Re electronic structure differences between the anions (**4** and **5**) and dimer **3** are negligible (Figure 2; Supporting Information, Figure S4). Therefore, a very similar amount of electron density lies on the metal center in the anions as in the dimer. Charge-density difference plots (obtained from restricted gas phase DFT-B3LYP[11] calculations using the LANL2DZ effective core potential and basis set with 15 explicit electrons on the Re,[12] the 6-31$^+$G**[13] basis set on all other atoms, and calculated with GAMESS-US[14]) show this result as well (Figure 4). Here, the red (dark) regions of the density difference show the unique orbital space of the HOMO of the [Re(bpy)(CO)$_3$]$^-$ anion is clearly delocalized across both the Re center and the bpy ligand. The purple (light) regions depict polarization of the complex after adding two electrons to the [Re(bpy)(CO)$_3$]$^+$ cation. These features are robust with respect to whether the anionic state is calculated as a closed-shell singlet or as an open-shell singlet (see the Supporting Information).

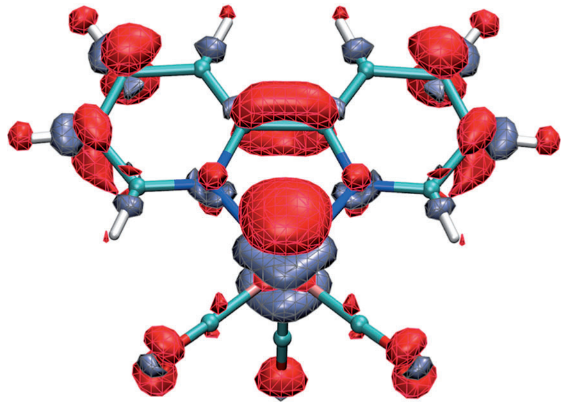

Figure 4. Density difference plots showing the polarization that occurs upon adding two electrons to the LUMO of the [Re(bpy)(CO)$_3$]$^+$ cation to form the HOMO of the [Re(bpy)(CO)$_3$]$^-$ anion. The isosurface depicts contour values of 0.005; red is increased charge density; purple is decreased charge density.

Figure 3 shows the area of the peak is smaller (ca. 50%) for $\mu(\mathbf{1})-\mu(\mathbf{4})$ than for the transfer of a single electron into Re 5d states ($\mu(\mathbf{6})-\mu(\mathbf{7})$). The same observation can also be made for the reduction of the Re^{+I} species **1** to dimer **3**. Therefore, the first reduction step from **1**→**3** involves a portion of the electronic charge stored in a bpy π* orbital that weakly overlaps with Re 5d orbitals. In a simplified view, the ground states of the anionic species (**4** and **5**) are best described formally as Re^0(bpy$^-$), rather than Re^{+I}(bpy^{2-}) or Re^{-I}(bpy^0). This formally places one electron in a Re d$_{z^2}$ orbital and one in the bpy π* orbital. These catalysts have been shown to react about 20 times faster with CO$_2$ than with H$^+$.[3b] The Re^0(bpy$^-$) ground state appears to be an electronic configuration which is favorable for engaging CO$_2$ preferentially over H$^+$ because engaging CO$_2$ involves transferring two electronic charges through both σ and π interactions, whereas engaging H$^+$ involves only a σ (Re d$_{z^2}$ + H 1s) interaction. This ground state is, by all appearances, a closed-shell singlet, showing no evidence of paramagnetism in room-temperature NMR spectra or from spin-polarized quantum mechanics calculations (where the closed-shell singlet state is favored over the triplet state by 0.79 eV in gas phase and 0.65 eV in acetonitrile solution; see the Supporting Information). The singlet nature of this ground state implies some long range coupling of the Re and bpy orbitals (overlapping tails of the wavefunctions would favor the singlet).

We previously characterized the structures of **1**, **2**, **4**, and **5** using XRD, but these results may not necessarily be valid for in situ catalysis. For instance, under ambient conditions, the catalyst could become coordinated with solvent molecules. However, EXAFS at the Re L_3 edge of complexes **1**, **2**, **4**, and **5** in frozen THF confirms that the XRD results accurately represent the coordination of the active catalyst. The solubility of the dimer **3** was too low to collect reliable data with the available experimental time. Quantitative results of EXAFS analysis for complexes **1**, **2**, **4**, and **5** are listed in the Supporting Information, Table S3.

Bond lengths and coordination around the metal centers obtained from the frozen-solution EXAFS agree with XRD structures previously reported,[3a,b,9] as well as the structures obtained in our and Fujita and Muckerman's DFT calculations.[8] Table 2 compares data from EXAFS and XRD experiments showing coordination numbers and bond lengths. (Individual scattering paths that contribute to the

Fourier transformed EXAFS data for complex **1** are shown in the Supporting Information, Figure S5; Fourier-transformed EXAFS data and fittings for complexes **1**, **2**, **4**, and **5**: Figures S6, S7; EXAFS data and fittings displayed in *k*-space: Figures S8, S9). From the EXAFS data we can conclude that the anions **4** and **5** remain five-coordinate in solution with no detectable coordination of solvent and no dimer formation.

In summary, we have applied experimental spectroscopy (IR, XANES, and EXAFS) and computational quantum chemistry (KS-DFT) to study the electronic structures and local coordination environments of catalytically relevant Re complexes and their reactive anions. XANES spectra of standards [Re(CO)$_5$Cl] (**6**) and [Re$_2$(CO)$_{10}$] (**7**) as well as a synthesized Re^{-I} anion, [K([18]crown-6)][Re(CO)$_5$] (**8**), have given us three distinct Re oxidation states for comparison with these catalytically relevant Re complexes. In terms of simplified formal charges, the anions [Re(bpy)(CO)$_3$]$^-$ (**4**) and [Re(bpy-*t*Bu)(CO)$_3$]$^-$ (**5**) are best described as possessing formally Re^0(bpy$^-$) ground states. The anions **4** and **5** are five-coordinate in solution with no coordination of solvent or dimer formation, which is consistent with XRD structures obtained in previous experiments.[3a,b,9]

The findings reported herein, together with recently reported stopped-flow kinetics studies of the anion, [Re(bpy-*t*Bu)(CO)$_3$]$^-$ (**5**), with CO$_2$ and weak acids,[3b] explain the high selectivity of the [Re(bpy)(CO)$_3$Cl] family of catalysts for the reduction of CO$_2$ in the presence of significant concentrations of H$^+$ sources. In general, the reduction of H$^+$ to H$_2$ is favored thermodynamically by 0.1 V over the reduction of CO$_2$ to CO, and so any catalyst that reduces CO$_2$ selectively in the presence of H$^+$ must do so on a kinetic basis with origins in the particular electronic structure of the catalyst. The formally Re^0(bpy$^-$) state found for these anions places one electron in a Re d$_{z^2}$ orbital, and one in the bpy π* orbital. It appears that this is an electronic configuration which is favorable for engaging CO$_2$ preferentially over H$^+$, and one that provides a lower reorganization energy for transferring two electronic charges to CO$_2$ through both σ and π interactions, compared to H$^+$, which could only involve σ (Re d$_{z^2}$ + H 1s) interaction. These findings may provide principles useful in the design of future catalysts for both carbon dioxide and proton reduction. Mechanistic investigations are underway to understand the complete CO$_2$ reduction process with these catalysts.

Received: December 11, 2012
Revised: February 6, 2013
Published online: March 25, 2013

Keywords: EXAFS · homogeneous catalysis · non-innocent ligands · rhenium · XANES

---

[1] E. E. Benson, C. P. Kubiak, A. J. Sathrum, J. M. Smieja, *Chem. Soc. Rev.* **2009**, *38*, 89–99.

[2] a) J.-M. Savéant, *Chem. Rev.* **2008**, *108*, 2348–2378; b) C. D. Windle, R. N. Perutz, *Coord. Chem. Rev.* **2012**, *256*, 2562–2570; c) M. Schulz, M. Karnahl, M. Schwalbe, J. G. Vos, *Coord. Chem. Rev.* **2012**, *256*, 1682–1705; d) Y. Tsuji, T. Fujihara, *Chem. Commun.* **2012**, *48*, 9956–9964; e) B. Kumar, M. Llorente, J. Froehlich, T. Dang, A. Sathrum, C. P. Kubiak, *Annu. Rev. Phys. Chem.* **2012**, *63*, 541–569; f) J. Schneider, H. Jia, J. T. Muckerman, E. Fujita, *Chem. Soc. Rev.* **2012**, *41*, 2036–2051; g) C. Finn, S. Schnittger, L. J. Yellowlees, J. B. Love, *Chem. Commun.* **2012**, *48*, 1392–1399; h) W. Wang, S. Wang, X. Ma, J. Gong, *Chem. Soc. Rev.* **2011**, *40*, 3703–3727; i) M. Mikkelsen, M. Jorgensen, F. C. Krebs, *Energy Environ. Sci.* **2010**, *3*, 43–81.

[3] a) E. E. Benson, C. P. Kubiak, *Chem. Commun.* **2012**, *48*, 7374–7376; b) J. M. Smieja, E. E. Benson, B. Kumar, K. A. Grice, C. S. Seu, A. J. M. Miller, J. M. Mayer, C. P. Kubiak, *Proc. Natl. Acad. Sci. USA* **2012**, *109*, 15646–15650; c) A. J. Morris, G. J. Meyer, E. Fujita, *Acc. Chem. Res.* **2009**, *42*, 1983–1994; d) J. M. Smieja, C. P. Kubiak, *Inorg. Chem.* **2010**, *49*, 9283–9289.

[4] E. Gore-Randall, M. Irwin, M. S. Denning, J. M. Goicoechea, *Inorg. Chem.* **2009**, *48*, 8304–8316.

[5] C. C. Scarborough, S. Sproules, T. Weyhermüller, S. DeBeer, K. Wieghardt, *Inorg. Chem.* **2011**, *50*, 12446–12462.

[6] a) C. A. Lippert, K. Riener, J. D. Soper, *Eur. J. Inorg. Chem.* **2012**, 554–561; b) W. Kaim, *Eur. J. Inorg. Chem.* **2012**, 343–348; c) B. de Bruin, E. Bill, E. Bothe, T. Weyhermüller, K. Wieghardt, *Inorg. Chem.* **2000**, *39*, 2936–2947; d) G. H. Spikes, C. Milsmann, E. Bill, T. Weyhermüller, K. Wieghardt, *Inorg. Chem.* **2008**, *47*, 11745–11754.

[7] F. Hartl, B. D. Rossenaar, G. J. Stor, D. J. Stufkens, *Recl. Trav. Chim. Pays-Bas* **1995**, *114*, 565–570.

[8] E. Fujita, J. T. Muckerman, *Inorg. Chem.* **2004**, *43*, 7636–7647.

[9] a) P. Kurz, B. Probst, B. Spingler, R. Alberto, *Eur. J. Inorg. Chem.* **2006**, 2966–2974; b) V. Yam, V. Lau, K. Cheung, *Organometallics* **1995**, *14*, 2749–2753.

[10] a) M. Fröba, K. Lochte, W. Metz, *J. Phys. Chem. Solids* **1996**, *57*, 635–641; b) A. Tougerti, S. Cristol, E. Berrier, V. Briois, C. La Fontaine, F. Villain, Y. Joly, *Phys. Rev. B* **2012**, *85*, 125136.

[11] a) C. Lee, W. Yang, R. G. Parr, *Phys. Rev. B* **1988**, *37*, 785–789; b) A. D. Becke, *Phys. Rev. A* **1988**, *38*, 3098–3100.

[12] P. J. Hay, W. R. Wadt, *J. Chem. Phys.* **1985**, *82*, 299–310.

[13] P. C. Hariharan, J. A. Pople, *Theor. Chim. Acta* **1973**, *28*, 213–222.

[14] a) M. W. Schmidt, K. K. Baldridge, J. A. Boatz, S. T. Elbert, M. S. Gordon, J. H. Jensen, S. Koseki, N. Matsunaga, K. A. Nguyen, S. Su, T. L. Windus, M. Dupuis, J. A. Montgomery, *J. Comput. Chem.* **1993**, *14*, 1347–1363; b) M. W. Gordon, M. W. Schmidt *Theory and Applications of Computational Chemistry: The First Forty Years*, Elsevier Science, Amsterdam, **2005**.

© 2013 Wiley-VCH Verlag GmbH & Co. KGaA, Weinheim